

Many-body k -local ground states as probes for unitary quantum metrology

Majid Hassani,^{1,2,*} Mengyao Hu,^{1,2,*} Guillem Müller-Rigat,^{3,*} Matteo Fadel,^{4,†} and Jordi Tura^{1,2,‡}

¹*Instituut-Lorentz, Universiteit Leiden, P.O. Box 9506, 2300 RA Leiden, The Netherlands*

² *$\langle aQa^L \rangle$ Applied Quantum Algorithms Leiden, The Netherlands*

³*Faculty of Physics, Astronomy and Applied Computer Science,*

Jagiellonian University, ul. Łojasiewicza 11, 30-348 Kraków, Poland

⁴*Department of Physics, ETH Zurich, 8093 Zurich, Switzerland*

(Dated: December 3, 2025)

Multipartite quantum states saturating the Heisenberg limit of sensitivity typically require full-body correlators to be prepared. On the other hand, experimentally practical Hamiltonians often involve few-body correlators only. Here, we study the metrological performances under this constraint, using tools derived from the quantum Fisher information. Our work applies to any encoding generator, also including a dependence on the parameter. We find that typical random symmetric ground states of k -body permutation-invariant Hamiltonians exhibit Heisenberg scaling. Finally, we establish a tradeoff between the Hamiltonian's gap, which quantifies preparation hardness, and the quantum Fisher information of the corresponding ground state.

The use of a quantum system for estimating an unknown parameter lies at the heart of quantum metrology and sensing [1–8], which form one of the foundational pillars of emerging quantum technologies [9]. Leveraging quantum resources, such as quantum correlations, can enhance the precision of parameter estimation beyond what is achievable by classical means. In parallel with extensive experimental progress [10–13], theoretical investigations, including both analytical [14–22] and numerical approaches [23–27], aim to identify optimal schemes that attain the fundamental limits of precision imposed by quantum mechanics.

A general quantum metrology protocol can be decomposed into three essential stages: (i) preparation of the probe state on which the parameter of interest is encoded, (ii) actual encoding of the unknown parameter through interaction with the probe, and (iii) measurement of the probe state after encoding to extract information about the parameter [1]. Here, we focus on the first stage. Determining the best probe is a crucial step, as it sets an upper bound on the precision achievable in the metrological task, which is given by the quantum Fisher information [28]. Equally important, however, is to identify probe states that are feasible to prepare in the laboratory. In this direction, we explore the metrological usefulness of ground states of permutation-invariant (PI) Hamiltonians which involve only few-body interactions. This class of Hamiltonians include Lipkin-Meshkov-Glick (LMG) models [29], which are naturally realized in various platforms, including ultracold atomic ensembles [30]. Excellent experimental developments also enable the control of the interaction length in many-body systems such as ion crystals [31–35], Rydberg arrays [36], and atomic ensembles in optical cavities [37]. There, ground states can be prepared through adiabatic protocols [38, 39] as long as the Hamiltonian gap is not too small [40, 41]. In previous works [42, 43], a connection between Haar ran-

dom symmetric states and metrological usefulness was highlighted. However, such a connection applies only to the parameter-independent encoding, and it requires Haar random states, which are notoriously difficult to prepare, even in the symmetric space, as they demand maximal complexity, *i.e.*, up to full system size interactions [44, 45].

In this work, we investigate *typical* metrological properties of ground states of random, physically-motivated Hamiltonians, which involve only k -local interactions. As a result, we show that, on average, these physically accessible ground states deliver close to maximal sensitivity, thus recovering the performance of Haar random symmetric states [42, 43]. We further reveal a tradeoff relation between the Hamiltonian's gap and the metrological usefulness of the corresponding ground state. We demonstrate that our results also apply to the case in which the encoding generator explicitly depends on the parameter, which remains much less explored, both in theory [19, 46, 47] and experiment [48, 49].

Preliminaries—In order to estimate the unknown parameter θ , one can prepare a probe quantum state, ρ_0 , on which the parameter is imprinted as $\rho_0 \rightarrow \rho_\theta$ via quantum dynamics. Performing a measurement on the evolved probe state, ρ_θ , provides information about θ . In quantum metrology, the fundamental bound on the attainable precision in estimating the unknown parameter θ for a given statistical model ρ_θ , can be addressed by the Cramér-Rao bound [1, 2, 28, 50]

$$\delta\theta \geq \frac{1}{\sqrt{\mathcal{F}[\theta]}}, \quad (1)$$

in which $\delta\theta$ represents the estimation error and $\mathcal{F}[\theta]$ is the quantum Fisher information (QFI) which quantifies the maximum amount of extractable information about the unknown parameter θ over all possible measurements

^{*}These authors contributed equally to this work.

[†]Present address: Institute for Quantum Computing, University of Waterloo, Waterloo, ON N2L 3G1, Canada.

[‡]Present address: Department of Physics, University of Valencia, 46100 Valencia, Spain.

and is a function of the final state ρ_θ . In this work we focus on pure probes $\rho_\theta = |\psi_\theta\rangle\langle\psi_\theta|$ that depend continuously on θ . Under this condition, the QFI can be expressed as

$$\mathcal{F}[|\psi_\theta\rangle] = 4(\langle\partial_\theta\psi_\theta|\partial_\theta\psi_\theta\rangle - \langle\psi_\theta|\partial_\theta\psi_\theta\rangle\langle\partial_\theta\psi_\theta|\psi_\theta\rangle). \quad (2)$$

Importantly, if the parameter encoding results from a unitary evolution, i.e. $|\psi_\theta\rangle = \mathbf{U}_\theta|\psi_0\rangle$, we can write $|\partial_\theta\psi_\theta\rangle = -i\mathbf{K}_\theta|\psi_\theta\rangle$, with the Hermitian operator $\mathbf{K}_\theta = i(\partial_\theta\mathbf{U}_\theta)\mathbf{U}_\theta^\dagger$. Eq. (2) thus simplifies to

$$\mathcal{F}[|\psi_\theta\rangle] = 4\Delta^2\mathbf{K}_\theta = 4(\langle\psi_\theta|\mathbf{K}_\theta^2|\psi_\theta\rangle - \langle\psi_\theta|\mathbf{K}_\theta|\psi_\theta\rangle^2). \quad (3)$$

Furthermore, we consider a system composed of N -qubits in which the parameter is imprinted identically in each qubit, $\mathbf{U}_\theta = U_\theta^{\otimes N}$, with $U_\theta = e^{-iG_\theta}$ in which G_θ denotes the generator of the unitary evolution. For such a case,

$$\mathcal{F}[|\psi_\theta\rangle] \leq N^2\|K_\theta\|_{\text{sn}}^2, \quad (4)$$

where $\|K_\theta\|_{\text{sn}} = \lambda_M(K_\theta) - \lambda_m(K_\theta)$ denotes the operator seminorm of Hermitian operator $K_\theta = i(\partial_\theta U_\theta)U_\theta^\dagger$, and λ_M/m represents the max/min eigenvalue, see Supplementary Material (SM) for derivation. The bound Eq. (4) can be saturated by the GHZ-type state $|\psi_\theta\rangle = (|\lambda_M(\theta)\rangle^{\otimes N} + |\lambda_m(\theta)\rangle^{\otimes N})/\sqrt{2}$, where $|\lambda_{M/m}(\theta)\rangle$ are respectively the max/min eigenvectors of K_θ . Unlike the ground states considered here, GHZ states are particularly demanding to prepare and because they require full-body interactions.

In order to analyze the behavior of the QFI with the number of particles N , we face an exponential growth of the Hilbert space dimension. To address this challenge, we derive an expression for the QFI for pure probe states $|\psi_0\rangle^{\text{sym.}} \in \mathcal{S}[(\mathbb{C}^2)^{\otimes N}]$ belonging to the symmetric subspace $\mathcal{S}[(\mathbb{C}^2)^{\otimes N}]$, which is spanned by the Dicke states $\{|D_N^n\rangle \propto |0\rangle^{\otimes n} \otimes |1\rangle^{\otimes (N-n)} + \text{perms.}\}$, where perms. indicates unique permutations [51]. Under these restrictions, the QFI explicitly reads:

$$\mathcal{F}[|\psi_\theta\rangle^{\text{sym.}}] = 4 \sum_{m,n,l=0}^N \alpha_m^* \alpha_n (\partial_\theta C_{lm})^* \partial_\theta C_{ln} - 4 \left| \sum_{m,n,l=0}^N \alpha_m^* \alpha_n C_{lm}^* \partial_\theta C_{ln} \right|^2, \quad (5)$$

where $\alpha_n = \langle D_N^n | \psi_0 \rangle^{\text{sym.}}$ are the components of $|\psi_0\rangle^{\text{sym.}}$ in the Dicke basis and $C_{nm} = \langle D_N^n | \mathbf{U}_\theta | D_N^m \rangle$, see SM. Equation (5) implies that the QFI can be directly computed in the symmetric subspace. By working within the symmetric subspace, which has dimension $(N+1)$, we drastically reduce the computational

complexity, enabling efficient analysis even for large N . Even though the symmetric subspace is exponentially small compared to the total Hilbert space, $(\mathbb{C}^2)^{\otimes N}$, those states maximally metrologically useful are, in fact, symmetric [6, 42]. In the rest of our work we focus on this scenario and omit the label “sym.” for simplicity of notation.

System—As already mentioned, we aim to characterize the metrological usefulness of ground states of experimentally practical Hamiltonians. In this way, we define the system’s Hamiltonian as follows

$$H = \sum_{a+b+c=k} \Gamma_{abc} S_{abc}, \quad (6)$$

where $\Gamma_{abc} \in \mathbb{R}$ denotes the coefficients, and the operator S_{abc} represents all-to-all PI k -body interactions and is given by

$$S_{abc} = \frac{1}{k!} (\sigma_x^{\otimes a} \otimes \sigma_y^{\otimes b} \otimes \sigma_z^{\otimes c} \otimes \mathbb{1}^{\otimes (N-k)} + \text{perms.}), \quad (7)$$

in which $\sigma_{x,y,z}$ are the standard Pauli matrices and $\mathbb{1}$ is the identity matrix. Physical Hamiltonians usually involve only few-body interactions (low k). If the ground state of H is non-degenerated, then, it must be symmetric. On the other hand, if it is degenerated onto other PI sectors, one can consider $\tilde{H} = -\tilde{S}^2 + H$, where $\tilde{S}^2 = N + 2(S_{200} + S_{020} + S_{002})$ is the total spin. Note that by construction the ground state of \tilde{H} is fully symmetric because the total spin \tilde{S}^2 commutes with H which is PI and it is maximized for symmetric states. Next, we derive a recursive formula for computing k -body interactions from lower-order ones

$$\begin{aligned} S_{abc} &= \frac{1}{k} S_{ab(c-1)} S_{001} - \frac{(N-k+2)(c-1)}{4k(k-1)} S_{ab(c-2)} \\ &\quad + \frac{i}{2k} (a S_{(a-1)(b+1)(c-1)} - b S_{(a+1)(b-1)(c-1)}), \end{aligned} \quad (8)$$

From Eq. (8), H can be described efficiently in the symmetric subspace using dynamical programming techniques and its ground state can be computed for large system sizes N (see SM). The associated QFI is then evaluated efficiently from Eq. (5). This versatile computational tool has potential applications beyond quantum metrology, including the construction of Bell inequalities based on few-body correlators [52–56].

Results—We begin with the case in which the parameter is encoded linearly as a phase, and conventionally taken as the spin operator along the x -direction, $G_\theta = \theta\sigma_x/2$. The maximum QFI attainable in this setting is

the so-called Heisenberg limit (HL), $\mathcal{F}[|\psi_\theta\rangle] = N^2$ [see Eq. (4)]. In addition, whenever the QFI surpasses the standard quantum limit (SQL), $\mathcal{F}[|\psi_\theta\rangle] > N$, we can say that the quantum state ρ_θ allows for quantum-enhanced sensitivity through the presence of metrologically useful entanglement, since a QFI saturating the SQL can be achieved by classical means.

As a first example, let us consider two-body correlators, $k = 2$, and a Hamiltonian Eq. (6) with only nonzero coefficient $\Gamma_{001} = \gamma$, i.e.

$$\tilde{H} = -\vec{S}^2 + \gamma S_{001}. \quad (9)$$

This Hamiltonian is an instance of the celebrated LMG model [29]. For N even and $\gamma > 0$, the ground state of Eq. (9) is the balanced Dicke state $|D_N^{N/2}\rangle$, which display exceptional metrological properties with QFI equal to $N(N/2 + 1)$. For N odd and/or $\gamma \leq 0$, the ground state of \tilde{H} is degenerated also in the symmetric subspace. While the ground state subspace may contain metrologically useful states, distinguishing them from the less useful ones generally requires experimentally demanding many-body interactions to lift the degeneracy. As an example, for $\gamma < 0$ and N even, the ground subspace contains the classically correlated states $|0\rangle^{\otimes N}, |1\rangle^{\otimes N}$, as well as the GHZ, $(|0\rangle^{\otimes N} + |1\rangle^{\otimes N})/\sqrt{2}$, which is maximally metrologically useful [see discussion below Eq. (4)]. However, to single out the GHZ state, one needs to add N -body interactions $S_{N00} = \sigma_x^{\otimes N}$ to break the degeneracy. The metrological usefulness of *subspaces* can be certified with the tools developed in Ref. [57] (see also Ref. [58]). Here, we may focus only on the cases where the ground state is unique in the symmetric subspace, as it is guaranteed that it can be prepared from few-body observables alone.

In this work, we investigate how generic is metrologically useful entanglement among ground states of random physical Hamiltonians involving up to k -body interactions. To that end, we sample Γ_{abc} , with $a + b + c = k$, randomly from a normal distribution $\mathcal{N}(0, 1)$ (mean 0 and variance 1). Then, we analyze the distribution of QFI over such random ground states, which outlines which metrological power to expect for disordered systems with uncontrolled interactions' strength. We find that for (N odd, k even) the ground states of typical Hamiltonians of the form Eq. (6) are degenerated. For odd k , while the ground state is unique, our numerical exploration shows usefulness compatible with the SQL for low k . Let us now analyze the case (N even, k even), where the conclusion changes. The results are displayed in Fig. 1.

We observe that the average value of the QFI over even few-body interactions and even number of particles N is $N(N + 1)/3$ in the finite-size regime. This value was posited in Refs. [42, 43] as the average QFI over symmetric states distributed according to the Haar measure.

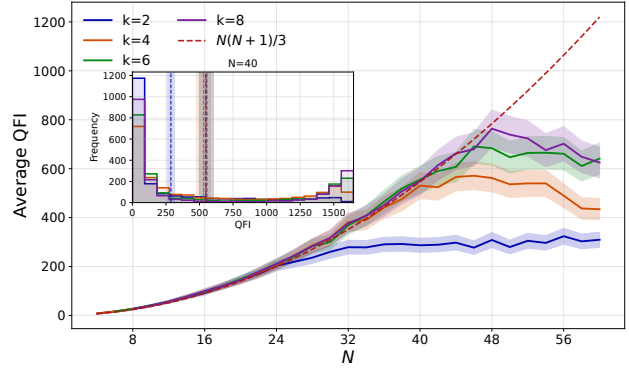


Figure 1. Average and fluctuations of the QFI as a function of N (even) over 2000 ground states of H , constructed with randomly sampled coefficients Γ_{abc} drawn from a normal distribution $\mathcal{N}(0, 1)$, for various k -body interactions. Solid curves denote sample averages; shaded regions indicate \pm standard error of the mean (SEM). The red dashed line shows the reference value $N(N + 1)/3$. Inset: Frequency histograms of the QFI at $N = 40$ for various k -body interactions. Vertical dashed lines mark the corresponding sample averages; light spans denote \pm SEM.

Conversely, as proven in these works, generic Haar multipartite states do not surpass the SQL, which motivates our choice of Hamiltonians with symmetric ground state Eq. (6). Symmetric Haar random states are notably difficult to produce as one expects that full-body interactions $k = N$ are needed for H to span the symmetric subspace. Specifically, according to Eq. (6), at least $(N+1)^2$ distinct k -body interactions terms are required to generate Haar-random states in the symmetric subspace. In comparison, the total number of k -body interactions appearing in Eq. (6) is $\sum_{k=0}^N \binom{k+2}{2} \in \mathcal{O}(N^3)$ while only $\mathcal{O}(N^2)$ of them are needed to achieve Haar randomness. Regarding this fact, we identify the smallest set of interactions needed to simulate Haar random ground states, which are presented in the End Matter. While these involve high order interactions, in Fig. 1 shows that, remarkably, for sufficiently low system's sizes, few-body interactions are sufficient to achieve the Haar random QFI bound. The inset Fig. 1 details the distribution of QFI over the physically accessible ground states. Interestingly, it resembles a bimodal distribution, where most samples show low QFI, while the few ones surpassing the SQL exhibit high QFI close to the HL.

Next, in order to further assess the preparation cost of such metrologically useful ground states, in Fig. (2) we plot the Hamiltonian's energy gap against the QFI for different random instances, $N = 10$ and $k = 2$. The energy gap $\lambda_{m+1}(H) - \lambda_m(H)$ (where λ_m, λ_{m+1} denotes the minimal and second minimal eigenvalue respectively) can be understood as a measure of preparation hardness. In order to compare different Hamiltoni-

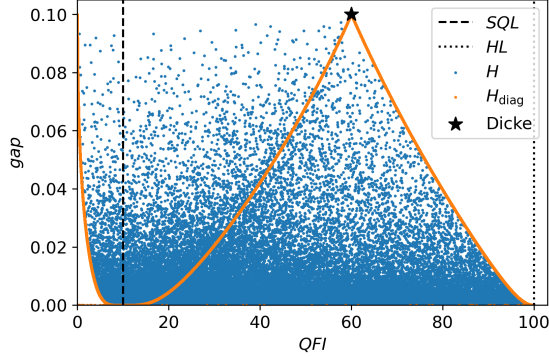


Figure 2. Energy gap and corresponding QFI for 10^5 ground states of random two-body Hamiltonians for $N = 10$ particles and $k = 2$, Eq. (6) (blue dots). Orange dots correspond to Hamiltonians with only nonzero coefficients, $\Gamma_{200}, \Gamma_{020}, \Gamma_{002}$. The star corresponds to Eq. (9), which displays a gap of $12/(N(N+2))$. Plots for higher k can be found at the End Matter.

ans, we normalize them such that $\langle H \rangle_0 = 0, \langle H \rangle_\infty = 1$, where $\langle H \rangle_T = \text{Tr}(He^{-H/T})/\text{Tr}(e^{-H/T})$ is the thermal expectation value.

In Fig. 2, we notice a tradeoff between the energy gap and the corresponding QFI: the highest the QFI, the narrowest is the energy gap of the corresponding Hamiltonian and the ground state becomes more difficult to prepare. The Hamiltonians which maximize the gap for a given QFI of the ground state are of the form $H_{\text{diag}} = \Gamma_{200}S_{200} + \Gamma_{020}S_{020} + \Gamma_{002}S_{002}$ (see orange line). In order to quantify this tradeoff for arbitrary system sizes, we can compute the line connecting the Dicke point $(12/(N(N+2)), N(N/2+1))$ (star in Fig. 2) and the Heisenberg point $(0, N^2)$, which upper-bounds the QFI for any even N as we verify numerically. From this observation, we arrive at $\mathcal{F}[\psi_0] \leq N^2 - N^2(N^2 - 4) \times \text{gap}/24$ for ground states $|\psi_0\rangle$ of Eq. (6) and $k = 2$. The fact that the QFI is maximized in critical systems, where the gap is closed, was already observed for certain models [59], while here we provide a more general bound.

In addition, the powerful tools we have developed for calculating Hamiltonians with k -body interactions in the symmetric subspace allows us to address nonlinear Hamiltonians, such as interacting encoding Hamiltonians. However, due to the ambiguity in resource accounting [60, 61] and in defining metrological advantage for nonlinear (as opposed to linear) Hamiltonians [43], we do not consider them further in this paper. Rather, we consider the case when the generator G_θ depends on the parameter. For instance, we take $G_\theta = \cos(\theta)\sigma_z + \sin(\theta)\sigma_x$ for illustration purposes. Using Eq. (4), we derive the θ -independent bound $\mathcal{F}[\psi_\theta] \leq [2\sin(1)N]^2$,

and we demonstrate that this bound is saturated by our method, see SM.

Since the QFI is no longer continuous in this case [62], the results of Ref. [42] are not directly applicable. Instead, we employ our method to characterize how random ground states perform as probes relative to the upper bound. Figure 5 shows the outcome of randomly sampling the coefficients in Eq. (6) from a normal distribution $\mathcal{N}(0, 1)$. These results reveal that few-body interactions already suffice to reach HL scaling for moderate system sizes. In comparison with Fig. 1, the ratio between the Haar bound and the QFI upper bound $[2\sin(1)]^{-2} \approx 0.35$ is better than the first case $(N+1)/(3N) \approx 0.33$. As matter of future research, it would be relevant to determine the encoding operation that maximizes the metrological gain of such Haar random symmetric states.

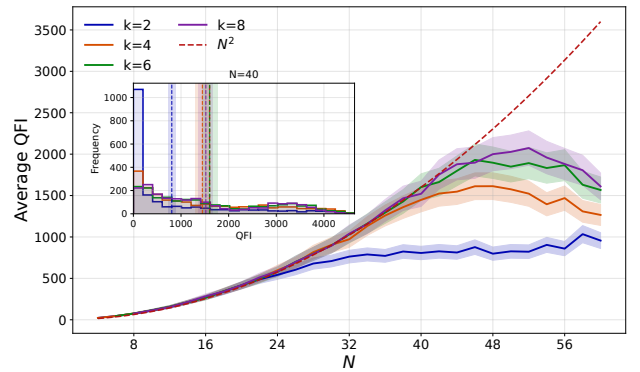


Figure 3. The QFI as a function of N for the encoding generator $K_\theta = \cos(\theta)\sigma_z + \sin(\theta)\sigma_x$ (cf. Fig. 1) for random θ . The probe states are the ground states of H , constructed with randomly sampled coefficients Γ_{abc} drawn from a normal distribution $\mathcal{N}(0, 1)$, for various k -body interactions. For each value of k , 2000 random instances were sampled.

Conclusions—In summary, we have studied the metrological usefulness of many-body ground states of PI Hamiltonians. As a result, we have found that typical random ground states of few-body PI Hamiltonians exhibit quantum-enhanced displaying Heisenberg scaling QFI. We have also identified minimal sets of interactions that are sufficient to simulate Haar random, metrologically useful ground states, and have characterized the distribution of Hamiltonians that lead to such advantage. Motivated by these findings, we have uncovered a tradeoff between the Hamiltonian’s gap, which quantifies preparation hardness, and the QFI of the corresponding ground state. As a byproduct of our findings, we have developed a dynamical programming algorithm that enables efficient evaluation of spin Hamiltonians in the symmetric subspace. Our work naturally opens up further research questions. In the context of

open quantum systems [63], it would be beneficial to characterize and analyze the preparation complexity [51] of the optimal probe state in more realistic scenarios, taking into consideration robustness against noise and/or particle losses. Another possible avenue for further research is to consider encoding generators beyond one-body interactions. Finally, the potential of the optimal probe states for revealing Bell correlations is a subject deserving further study [17, 64, 65].

Code and data statement— Code and data are available from the authors upon reasonable request.

Acknowledgments—We thank Jin-Fu Chen for insightful discussions on the computation of k -body interactions in the symmetric subspace. Majid Hassani and JT acknowledge the support received from the European Union’s Horizon Europe research and innovation programme through the ERC StG FINE-TEA-SQUAD (Grant No. 101040729). This publication is part of the ‘Quantum Inspire - the Dutch Quantum Computer in the Cloud’ project (with project number [NWA.1292.19.194]) of the NWA research program ‘Research on Routes by Consortia (ORC)’, which is funded by the Netherlands Organization for Scientific Research (NWO). GMR acknowledges financial support by the European Union under ERC Advanced Grant TAtypic, Project No. 101142236. MF was supported by the Swiss National Science Foundation Ambizione Grant No. 208886, and by The Branco Weiss Fellowship – Society in Science, administered by the ETH Zürich. Views and opinions expressed are, however, those of the author(s) only and do not necessarily reflect those of the funding institutions. Neither of the funding institutions can be held responsible for them.

P. Treutlein, Quantum metrology with nonclassical states of atomic ensembles, *Reviews of Modern Physics* **90**, 035005 (2018).

- [7] E. Polino, M. Valeri, N. Spagnolo, and F. Sciarrino, Photonic quantum metrology, *AVS Quantum Science* **2**, 024703 (2020).
- [8] M. Fadel, N. Roux, and M. Gessner, Quantum metrology with a continuous-variable system, *Reports on Progress in Physics* **88**, 106001 (2025).
- [9] D. S. Simon, *Introduction to Quantum Science and Technology*, Undergraduate Texts in Physics (Springer Nature Switzerland, Cham, 2025).
- [10] E. Pedrozo-Peña, S. Colombo, C. Shu, A. F. Adiyatullin, Z. Li, E. Mendez, B. Braverman, A. Kawasaki, D. Akamatsu, Y. Xiao, and V. Vuletić, Entanglement on an optical atomic-clock transition, *Nature* **588**, 414 (2020).
- [11] C. Troullinou, V. G. Lucivero, and M. W. Mitchell, Quantum-Enhanced Magnetometry at Optimal Number Density, *Physical Review Letters* **131**, 133602 (2023).
- [12] C. Cassens, B. Meyer-Hoppe, E. Rasel, and C. Klemp, Entanglement-Enhanced Atomic Gravimeter, *Physical Review X* **15**, 011029 (2025).
- [13] L. Pezzè and A. Smerzi, *Advances in multiparameter quantum sensing and metrology* (2025).
- [14] R. Demkowicz-Dobrzański, J. Kołodyński, and M. Guja, The elusive Heisenberg limit in quantum-enhanced metrology, *Nature Communications* **3**, 1063 (2012).
- [15] R. Demkowicz-Dobrzański and L. Maccone, Using Entanglement Against Noise in Quantum Metrology, *Physical Review Letters* **113**, 250801 (2014).
- [16] M. Hassani, C. Macchiavello, and L. Maccone, Digital Quantum Estimation, *Physical Review Letters* **119**, 200502 (2017).
- [17] F. Fröwis, M. Fadel, P. Treutlein, N. Gisin, and N. Brunner, Does large quantum Fisher information imply Bell correlations?, *Physical Review A* **99**, 040101 (2019).
- [18] L. Pezzè and A. Smerzi, Heisenberg-Limited Noisy Atomic Clock Using a Hybrid Coherent and Squeezed State Protocol, *Physical Review Letters* **125**, 210503 (2020).
- [19] M. Annabestani, M. Hassani, D. Tamascelli, and M. G. A. Paris, Multiparameter quantum metrology with discrete-time quantum walks, *Physical Review A* **105**, 062411 (2022).
- [20] X. Lu, W. Górecki, C. Macchiavello, and L. Maccone, Number of bits returned by a quantum estimation, *Physical Review A* **110**, 032405 (2024).
- [21] S. Kurdzialek, W. Górecki, F. Albarelli, and R. Demkowicz-Dobrzański, Using Adaptiveness and Causal Superpositions Against Noise in Quantum Metrology, *Physical Review Letters* **131**, 090801 (2023).
- [22] M. Hassani, S. Scheiner, M. G. A. Paris, and D. Markham, Privacy in Networks of Quantum Sensors, *Physical Review Letters* **134**, 030802 (2025).
- [23] M. Jarzyna and R. Demkowicz-Dobrzański, Matrix Product States for Quantum Metrology, *Physical Review Letters* **110**, 240405 (2013).
- [24] K. Chabuda, J. Dziarmaga, T. J. Osborne, and R. Demkowicz-Dobrzański, Tensor-network approach for quantum metrology in many-body quantum systems, *Nature Communications* **11**, 250 (2020).

* These authors contributed equally to this work.

† fadelm@phys.ethz.ch

‡ tura@lorentz.leidenuniv.nl

- [1] V. Giovannetti, S. Lloyd, and L. Maccone, Quantum Metrology, *Physical Review Letters* **96**, 010401 (2006).
- [2] M. G. A. Paris, QUANTUM ESTIMATION FOR QUANTUM TECHNOLOGY, *International Journal of Quantum Information* **07**, 125 (2009).
- [3] V. Giovannetti, S. Lloyd, and L. Maccone, Advances in quantum metrology, *Nature Photonics* **5**, 222 (2011).
- [4] B. M. Escher, R. L. De Matos Filho, and L. Davidovich, General framework for estimating the ultimate precision limit in noisy quantum-enhanced metrology, *Nature Physics* **7**, 406 (2011).
- [5] C. L. Degen, F. Reinhard, and P. Cappellaro, Quantum sensing, *Reviews of Modern Physics* **89**, 035002 (2017).
- [6] L. Pezzè, A. Smerzi, M. K. Oberthaler, R. Schmied, and

[25] K. Chabuda and R. Demkowicz-Dobrzański, TNQMetro: Tensor-network based package for efficient quantum metrology computations, *Computer Physics Communications* **274**, 108282 (2022).

[26] S. Kurdzialek, P. Dulian, J. Majsa, S. Chakraborty, and R. Demkowicz-Dobrzański, Quantum metrology using quantum combs and tensor network formalism, *New Journal of Physics* **27**, 013019 (2025).

[27] P. Dulian, S. Kurdzialek, and R. Demkowicz-Dobrzański, QMetro++ – Python optimization package for large scale quantum metrology with customized strategy structures (2025).

[28] S. L. Braunstein and C. M. Caves, Statistical distance and the geometry of quantum states, *Physical Review Letters* **72**, 3439 (1994).

[29] H. Lipkin, N. Meshkov, and A. Glick, Validity of many-body approximation methods for a solvable model, *Nuclear Physics* **62**, 188 (1965).

[30] Y. Kawaguchi and M. Ueda, Spinor Bose–Einstein condensates, *Physics Reports* **520**, 253 (2012).

[31] C. Monroe, W. C. Campbell, L.-M. Duan, Z.-X. Gong, A. V. Gorshkov, P. W. Hess, R. Islam, K. Kim, N. M. Linke, G. Pagano, P. Richerme, C. Senko, and N. Y. Yao, Programmable quantum simulations of spin systems with trapped ions, *Reviews of Modern Physics* **93**, 025001 (2021).

[32] J. W. Britton, B. C. Sawyer, A. C. Keith, C.-C. J. Wang, J. K. Freericks, H. Uys, M. J. Biercuk, and J. J. Bollinger, Engineered two-dimensional Ising interactions in a trapped-ion quantum simulator with hundreds of spins, *Nature* **484**, 489 (2012).

[33] R. Islam, C. Senko, W. C. Campbell, S. Korenblit, J. Smith, A. Lee, E. E. Edwards, C.-C. J. Wang, J. K. Freericks, and C. Monroe, Emergence and Frustration of Magnetism with Variable-Range Interactions in a Quantum Simulator, *Science* **340**, 583 (2013).

[34] P. Jurcevic, B. P. Lanyon, P. Hauke, C. Hempel, P. Zoller, R. Blatt, and C. F. Roos, Quasiparticle engineering and entanglement propagation in a quantum many-body system, *Nature* **511**, 202 (2014).

[35] O. Katz, M. Cetina, and C. Monroe, Programmable N - Body Interactions with Trapped Ions, *PRX Quantum* **4**, 030311 (2023).

[36] F. M. Gambetta, C. Zhang, M. Hennrich, I. Lesanovsky, and W. Li, Long-Range Multibody Interactions and Three-Body Antiblockade in a Trapped Rydberg Ion Chain, *Physical Review Letters* **125**, 133602 (2020).

[37] A. Periwal, E. S. Cooper, P. Kunkel, J. F. Wienand, E. J. Davis, and M. Schleier-Smith, Programmable interactions and emergent geometry in an array of atom clouds, *Nature* **600**, 630 (2021).

[38] B. Evrard, A. Qu, J. Dalibard, and F. Gerbier, Observation of fragmentation of a spinor Bose-Einstein condensate, *Science* **373**, 1340 (2021).

[39] Y.-Q. Zou, L.-N. Wu, Q. Liu, X.-Y. Luo, S.-F. Guo, J.-H. Cao, M. K. Tey, and L. You, Beating the classical precision limit with spin-1 Dicke states of more than 10,000 atoms, *Proceedings of the National Academy of Sciences* **115**, 6381 (2018).

[40] K. S. Rai, I. Kull, P. Emonts, J. Tura, N. Schuch, and F. Baccari, *A Hierarchy of Spectral Gap Certificates for Frustration-Free Spin Systems* (2024).

[41] K. S. Rai, J.-F. Chen, P. Emonts, and J. Tura, Spectral Gap Optimization for Enhanced Adiabatic State Preparation, *Physical Review Letters* **135**, 090602 (2025).

[42] M. Oszmaniec, R. Augusiak, C. Gogolin, J. Kołodyński, A. Acín, and M. Lewenstein, Random Bosonic States for Robust Quantum Metrology, *Physical Review X* **6**, 041044 (2016).

[43] S. Imai, A. Smerzi, and L. Pezzè, Metrological usefulness of entanglement and nonlinear Hamiltonians, *Physical Review A* **111**, L020402 (2025).

[44] D. Gross, K. Audenaert, and J. Eisert, Evenly distributed unitaries: On the structure of unitary designs, *Journal of Mathematical Physics* **48**, 052104 (2007).

[45] H. Zhu, R. Kueng, M. Grassl, and D. Gross, *The Clifford group fails gracefully to be a unitary 4-design* (2016).

[46] S. Pang and T. A. Brun, Quantum metrology for a general Hamiltonian parameter, *Physical Review A* **90**, 022117 (2014).

[47] S. Pang and A. N. Jordan, Optimal adaptive control for quantum metrology with time-dependent Hamiltonians, *Nature Communications* **8**, 14695 (2017).

[48] H. Souquet-Basiègue, B. Roussel, G. Rebora, G. Ménard, I. Safi, G. Fève, and P. Degiovanni, Quantum Sensing of Time-Dependent Electromagnetic Fields with Single-Electron Excitations, *Physical Review X* **15**, 031043 (2025).

[49] C. H. Alderete, A. K. Srivastava, and A. T. Sornborger, *Nonlinear Quantum Sensing with a Frustrated Kitaev Trimer* (2025).

[50] S. L. Braunstein, C. M. Caves, and G. Milburn, Generalized Uncertainty Relations: Theory, Examples, and Lorentz Invariance, *Annals of Physics* **247**, 135 (1996).

[51] C. Marconi, G. Müller-Rigat, J. Romero-Pallejà, J. Tura, and A. Sanpera, *Symmetric quantum states: A review of recent progress* (2025).

[52] J. Tura, R. Augusiak, A. B. Sainz, T. Vértesi, M. Lewenstein, and A. Acín, Detecting nonlocality in many-body quantum states, *Science* **344**, 1256 (2014).

[53] J. Tura, R. Augusiak, A. Sainz, B. Lücke, C. Klemp, M. Lewenstein, and A. Acín, Nonlocality in many-body quantum systems detected with two-body correlators, *Annals of Physics* **362**, 370 (2015).

[54] A. Aloy, G. Müller-Rigat, J. Tura, and M. Fadel, Deriving Three-Outcome Permutationally Invariant Bell Inequalities, *Entropy* **26**, 816 (2024).

[55] G. Müller-Rigat, A. Aloy, M. Lewenstein, and I. Frerot, Inferring Nonlinear Many-Body Bell Inequalities From Average Two-Body Correlations: Systematic Approach for Arbitrary Spin- j Ensembles, *PRX Quantum* **2**, 030329 (2021).

[56] G. Müller-Rigat, A. Aloy, M. Lewenstein, M. Fadel, and J. Tura, *Three-outcome multipartite Bell inequalities: Applications to dimension witnessing and spin-nematic squeezing in many-body systems* (2024).

[57] G. Müller-Rigat, A. K. Srivastava, S. Kurdzialek, G. Rajchel-Mieldzioć, M. Lewenstein, and I. Frerot, Certifying the quantum Fisher information from a given set of mean values: A semidefinite programming approach, *Quantum* **7**, 1152 (2023).

[58] I. Frerot and T. Roscilde, *Symmetry: A Fundamental Re-*

source for Quantum Coherence and Metrology, [Physical Review Letters 133, 260402 \(2024\)](#).

[59] I. Frerot and T. Roscilde, Quantum Critical Metrology, [Physical Review Letters 121, 020402 \(2018\)](#).

[60] M. Zwierz, C. A. Pérez-Delgado, and P. Kok, General Optimality of the Heisenberg Limit for Quantum Metrology, [Physical Review Letters 105, 180402 \(2010\)](#).

[61] M. Zwierz, C. A. Pérez-Delgado, and P. Kok, Ultimate limits to quantum metrology and the meaning of the Heisenberg limit, [Physical Review A 85, 042112 \(2012\)](#).

[62] A. T. Rezakhani, M. Hassani, and S. Alipour, Continuity of the quantum Fisher information, [Physical Review A 100, 032317 \(2019\)](#).

[63] S. Kurdzialek, F. Albarelli, and R. Demkowicz-Dobrzański, Universal Bounds for Quantum Metrology in the Presence of Correlated Noise, [Physical Review Letters 135, 130801 \(2025\)](#).

[64] A. Niezgoda and J. Chwedeczuk, Many-Body Nonlocality as a Resource for Quantum-Enhanced Metrology, [Physical Review Letters 126, 210506 \(2021\)](#).

[65] I. Frerot, M. Fadel, and M. Lewenstein, Probing quantum correlations in many-body systems: A review of scalable methods, [Reports on Progress in Physics 86, 114001 \(2023\)](#).

[66] A. A. Mele, Introduction to Haar Measure Tools in Quantum Information: A Beginner's Tutorial, [Quantum 8, 1340 \(2024\)](#).

[67] S. Boixo, S. T. Flammia, C. M. Caves, and J. Geremia, Generalized Limits for Single-Parameter Quantum Estimation, [Physical Review Letters 98, 090401 \(2007\)](#).

End Matter

CONSTRUCTING HAAR-RANDOM STATES FROM SYSTEM HAMILTONIAN

As discussed in the main text, the coefficients Γ_{abc} in the system Hamiltonian

$$H = \sum_{a,b,c=1}^{k \leq N} \Gamma_{abc} S_{abc}, \quad (10)$$

are chosen randomly. For a given N , each of k -body interaction terms S_{abc} is represented by an $(N+1) \times (N+1)$ matrix. The number of distinct k -body interactions is given by $\binom{k+2}{k} = (k+2)(k+1)/2$. Hence, the total number of interaction terms appearing in Eq. (10) is

$$\begin{aligned} N &= \sum_{k=0}^N \binom{k+2}{2} = \sum_{k=0}^N \frac{(k+2)(k+1)}{2} \\ &= \frac{(N+3)(N+2)(N+1)}{6} \in \mathcal{O}(N^3). \end{aligned} \quad (11)$$

The vectorized form of Eq. (10) can be expressed as

$$|H\rangle\langle = \mathcal{S}|\Gamma\rangle\langle, \quad (12)$$

where $|\circ\rangle\langle$ denotes the vectorization of \circ and \mathcal{S} is an $(N+1)^2 \times N$ matrix whose columns correspond to the vectorized interaction terms $|S_{abc}\rangle\langle$. By randomly sampling the components of $|\Gamma\rangle\langle$, a random vector $|H\rangle\langle$ is generated. Since in general $N \neq (N+1)^2$, an important question arises: *What is the minimum number of k -body interaction terms required to construct a Haar-random state $|H\rangle\langle$?*

To address this question, let us recall the concept of a multivariate normal vector. A random vector $\mathbf{X} = (X_1, X_2, \dots, X_k)^T$ is said to follow a multivariate normal distribution if it can be written as

$$\mathbf{X} = \mathbf{A}\mathbf{Z} + \mu, \quad (13)$$

where \mathbf{A} is a $k' \times l'$ matrix, $\mathbf{Z} = (Z_1, Z_2, \dots, Z_{l'})^T$, and $\mu \in \mathbb{R}^{k'}$. The associated covariance matrix is $\Sigma = \mathbf{A}\mathbf{A}^T$. If Σ is of full rank, then the columns of \mathbf{A} are linearly independent, and \mathbf{X} follows a genuine (non-degenerate) multivariate normal distribution supported on all of $\mathbb{R}^{k'}$.

Hence, we construct \mathcal{S}' by sequentially adding the vectorized interaction terms $|S_{abc}\rangle\langle$ until the covariance matrix $\Sigma = \mathcal{S}'\mathcal{S}'^T$ becomes full rank. Our numerical results indicate that, to obtain a full-rank covariance matrix Σ , at least $(N+1)^2$ distinct k -body interaction terms are required. Following is the list of numerical results

N	Final Rank $(N+1)^2$	Subset Size	Sufficient set of interaction terms
3	16	16	$1, S_{001}, S_{010}, S_{100}, S_{002}, S_{011}, S_{020}, S_{101}, S_{110}, S_{003}, S_{012}, S_{021}, S_{030}, S_{102}, S_{111}, S_{120}$
4	25	25	$1, S_{001}, S_{010}, S_{100}, S_{002}, S_{011}, S_{020}, S_{101}, S_{110}, S_{003}, S_{012}, S_{021}, S_{030}, S_{102}, S_{111}, S_{120}, S_{004}, S_{013}, S_{022}, S_{031}, S_{040}, S_{103}, S_{112}, S_{121}, S_{130}$
5	36	36	$1, S_{001}, S_{010}, S_{100}, S_{002}, S_{011}, S_{020}, S_{101}, S_{110}, S_{003}, S_{012}, S_{021}, S_{030}, S_{102}, S_{111}, S_{120}, S_{004}, S_{013}, S_{022}, S_{031}, S_{040}, S_{103}, S_{112}, S_{121}$

			$S_{130}, S_{005}, S_{014}, S_{023}, S_{032}, S_{041}, S_{050}, S_{104}, S_{113}, S_{122}, S_{131}, S_{140}$
6	49	49	$\mathbb{1}, S_{001}, S_{010}, S_{100}, S_{002}, S_{011}, S_{020}, S_{101}, S_{110}, S_{003}, S_{012}, S_{021}, S_{030}, S_{102}, S_{111}, S_{120}, S_{004}, S_{013}, S_{022}, S_{031}, S_{040}, S_{103}, S_{112}, S_{121}, S_{130}, S_{005}, S_{014}, S_{023}, S_{032}, S_{041}, S_{050}, S_{104}, S_{113}, S_{122}, S_{131}, S_{140}, S_{006}, S_{015}, S_{024}, S_{033}, S_{042}, S_{051}, S_{060}, S_{105}, S_{114}, S_{123}, S_{132}, S_{141}, S_{150}$
10	121	121	$\mathbb{1}, S_{001}, S_{010}, S_{100}, S_{002}, S_{011}, S_{020}, S_{101}, S_{110}, S_{003}, S_{012}, S_{021}, S_{030}, S_{102}, S_{111}, S_{120}, S_{004}, S_{013}, S_{022}, S_{031}, S_{040}, S_{103}, S_{112}, S_{121}, S_{130}, S_{005}, S_{014}, S_{023}, S_{032}, S_{041}, S_{050}, S_{104}, S_{113}, S_{122}, S_{131}, S_{140}, S_{006}, S_{015}, S_{024}, S_{033}, S_{042}, S_{051}, S_{060}, S_{105}, S_{114}, S_{123}, S_{132}, S_{141}, S_{150}, S_{007}, S_{016}, S_{025}, S_{034}, S_{043}, S_{052}, S_{061}, S_{070}, S_{106}, S_{115}, S_{124}, S_{133}, S_{142}, S_{151}, S_{160}, S_{008}, S_{017}, S_{026}, S_{035}, S_{044}, S_{053}, S_{062}, S_{071}, S_{080}, S_{107}, S_{116}, S_{125}, S_{134}, S_{143}, S_{152}, S_{161}, S_{170}, S_{009}, S_{018}, S_{027}, S_{036}, S_{045}, S_{054}, S_{063}, S_{072}, S_{081}, S_{090}, S_{108}, S_{117}, S_{126}, S_{135}, S_{144}, S_{153}, S_{162}, S_{171}, S_{180}, S_{010}, S_{019}, S_{028}, S_{037}, S_{046}, S_{055}, S_{064}, S_{073}, S_{082}, S_{091}, S_{100}, S_{109}, S_{118}, S_{127}, S_{136}, S_{145}, S_{154}, S_{163}, S_{172}, S_{181}, S_{190}$

QFI AND THE ENERGY GAP

In the following we present addition plots of the energy gap versus QFI for various order of interactions k (see Fig. 2 of the main text).

We notice that diagonal Hamiltonians (orange dots) cease to be optimal for $k > 2$. On the other hand, increasing the order of the interactions leads to a larger gap (notice y -axis scale), which facilitates the preparation of states with high QFI (see rightmost part of the plots). In the limiting case $k = N = 10$, diagonal Hamiltonians are degenerated, and, as expected, the tradeoff between the QFI and the gap imposed by the order of the interactions is lifted.

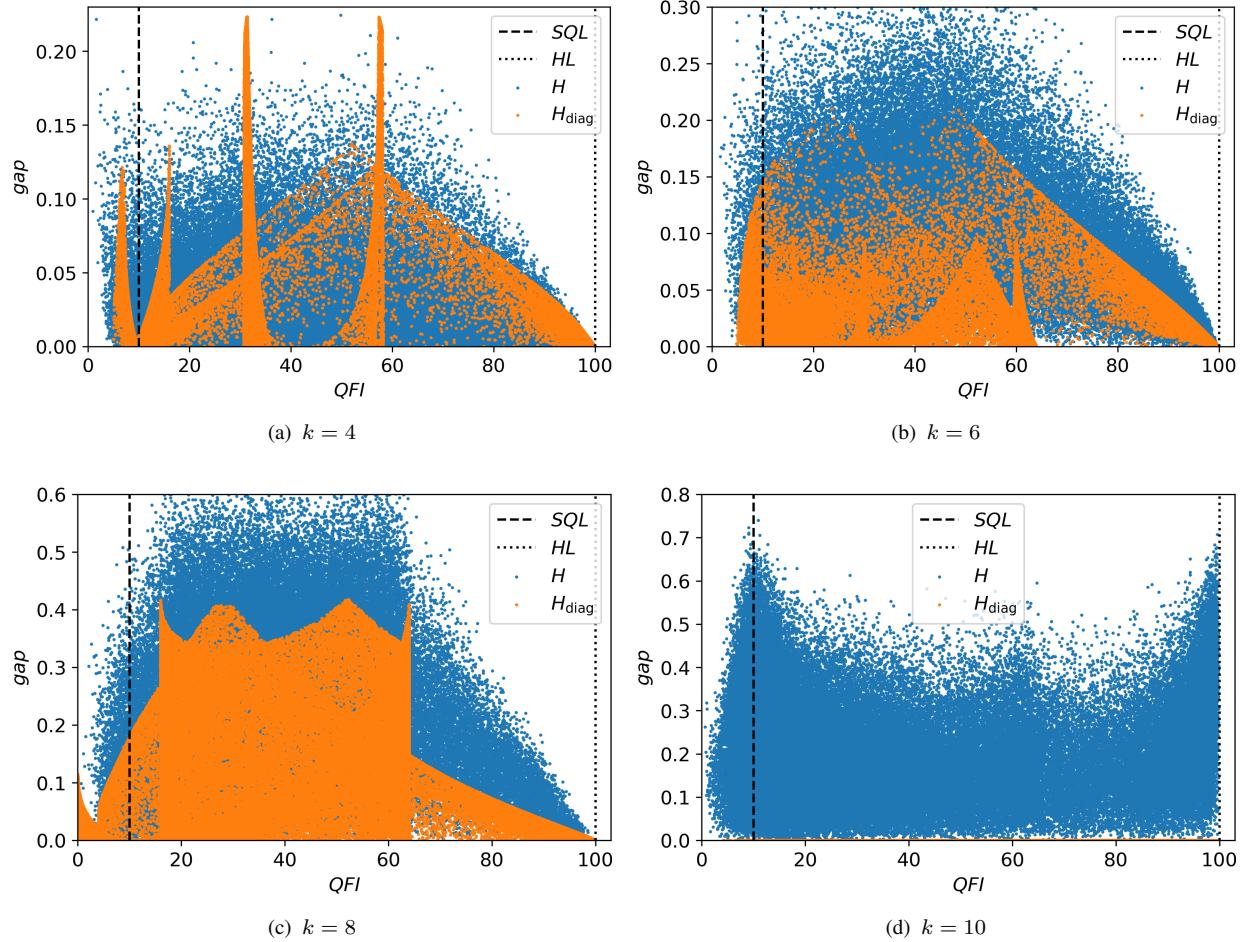


Figure 4. Energy gap and corresponding QFI for 10^5 ground states of random two-body Hamiltonians for $N = 10$ particles and different order of interactions k (blue dots). Orange dots correspond to Hamiltonians with only nonzero coefficients, $\Gamma_{k00}, \Gamma_{0k0}, \Gamma_{00k}$.

SUPPLEMENTARY MATERIAL

COMPUTING THE PI k -BODY INTERACTION TERMS IN THE SYMMETRIC SUBSPACE

We present a recursive formula for computing the PI k -body interaction terms in the symmetric subspace. Let us first introduce the one-body interaction terms as follows

$$S_\mu = \sum_{i=1}^N \frac{1}{2} \sigma_\mu^{(i)}, \quad (14)$$

where N is the number of sites (observers in the multipartite Bell experiment) and $\frac{1}{2} \sigma_\mu^{(i)}$ ($\mu \in \{x, y, z\}$) represents the tensor product of the Pauli matrix $\frac{1}{2} \sigma_\mu$ acting at the i -th site, with identity matrices elsewhere. It is straightforward to check that the one-body interaction terms satisfy the following commutation relations

$$[S_x, S_y] = iS_z, \quad [S_y, S_z] = iS_x, \quad [S_z, S_x] = iS_y. \quad (15)$$

Equation (14) can be generalized to define the k -body interaction terms as

$$S_{\mu_1 \mu_2 \dots \mu_k} = \frac{1}{k!} \sum_{i_1 \neq i_2 \neq \dots \neq i_k=1}^N \frac{1}{2} \sigma_{\mu_1}^{(i_1)} \otimes \frac{1}{2} \sigma_{\mu_2}^{(i_2)} \otimes \dots \otimes \frac{1}{2} \sigma_{\mu_k}^{(i_k)}. \quad (16)$$

In order to find a recursive relation to computing k -body interaction terms from lower-order interaction terms, let us begin from

$$\begin{aligned} & \left(\sum_{i_1 \neq i_2 \neq \dots \neq i_{k-1}=1}^N \frac{1}{2} \sigma_{\mu_1}^{(i_1)} \otimes \frac{1}{2} \sigma_{\mu_2}^{(i_2)} \otimes \dots \otimes \frac{1}{2} \sigma_{\mu_{k-1}}^{(i_{k-1})} \right) \left(\sum_{i_k=1}^N \frac{1}{2} \sigma_{\mu_k}^{(i_k)} \right) = \\ & \sum_{i_1 \neq i_2 \neq \dots \neq i_k=1}^N \frac{1}{2} \sigma_{\mu_1}^{(i_1)} \otimes \frac{1}{2} \sigma_{\mu_2}^{(i_2)} \otimes \dots \otimes \frac{1}{2} \sigma_{\mu_k}^{(i_k)} + \sum_{\substack{i_1 \neq i_2 \neq \dots \neq i_{k-1}=1 \\ i_1=i_k}}^N \frac{1}{4} \sigma_{\mu_1}^{(i_1)} \sigma_{\mu_k}^{(i_1)} \otimes \frac{1}{2} \sigma_{\mu_2}^{(i_2)} \otimes \dots \otimes \frac{1}{2} \sigma_{\mu_{k-1}}^{(i_{k-1})} \\ & + \sum_{\substack{i_1 \neq i_2 \neq \dots \neq i_{k-1}=1 \\ i_2=i_k}}^N \frac{1}{2} \sigma_{\mu_1}^{(i_1)} \otimes \frac{1}{4} \sigma_{\mu_1}^{(i_2)} \sigma_{\mu_k}^{(i_2)} \otimes \dots \otimes \frac{1}{2} \sigma_{\mu_{k-1}}^{(i_{k-1})} + \dots + \sum_{\substack{i_1 \neq i_2 \neq \dots \neq i_{k-1}=1 \\ i_{k-1}=i_k}}^N \frac{1}{2} \sigma_{\mu_1}^{(i_1)} \otimes \frac{1}{2} \sigma_{\mu_2}^{(i_2)} \otimes \dots \otimes \frac{1}{4} \sigma_{\mu_{k-1}}^{(i_{k-1})} \sigma_{\mu_k}^{(i_{k-1})}. \end{aligned} \quad (17)$$

The Pauli matrices satisfy

$$\sigma_\mu \sigma_\nu = \delta_{\mu\nu} \mathbb{1} + i \varepsilon_{\mu\nu\lambda} \sigma_\lambda, \quad (18)$$

where $\varepsilon_{\mu\nu\lambda}$ denotes the Levi-Civita symbol which is defined as follows: $\varepsilon_{xyz} = 1$ for even permutations of (x, y, z) , -1 for odd permutations, and 0 if any index is repeated. Applying Eq. (18) in Eq. (17), yields

$$\begin{aligned}
& \left(\sum_{i_1 \neq i_2 \neq \dots \neq i_{k-1}=1}^N \frac{1}{2} \sigma_{\mu_1}^{(i_1)} \otimes \frac{1}{2} \sigma_{\mu_2}^{(i_2)} \otimes \dots \otimes \frac{1}{2} \sigma_{\mu_{k-1}}^{(i_{k-1})} \right) \left(\sum_{i_k=1}^N \frac{1}{2} \sigma_{\mu_k}^{(i_k)} \right) = \\
& \sum_{i_1 \neq i_2 \neq \dots \neq i_k=1}^N \frac{1}{2} \sigma_{\mu_1}^{(i_1)} \otimes \frac{1}{2} \sigma_{\mu_2}^{(i_2)} \otimes \dots \otimes \frac{1}{2} \sigma_{\mu_k}^{(i_k)} + \sum_{\substack{i_1 \neq i_2 \neq \dots \neq i_{k-1}=1 \\ i_1=i_k}}^N \frac{1}{4} \left(\delta_{\mu_1 \mu_k} \mathbb{1} + i \varepsilon_{\mu_1 \mu_k \mu'} \sigma_{\mu'}^{(i_1)} \right) \otimes \frac{1}{2} \sigma_{\mu_2}^{(i_2)} \otimes \dots \otimes \frac{1}{2} \sigma_{\mu_{k-1}}^{(i_{k-1})} \\
& + \sum_{\substack{i_1 \neq i_2 \neq \dots \neq i_{k-1}=1 \\ i_2=i_k}}^N \frac{1}{2} \sigma_{\mu_1}^{(i_1)} \otimes \frac{1}{4} \left(\delta_{\mu_2 \mu_k} \mathbb{1} + i \varepsilon_{\mu_2 \mu_k \mu'} \sigma_{\mu'}^{(i_2)} \right) \otimes \dots \otimes \frac{1}{2} \sigma_{\mu_{k-1}}^{(i_{k-1})} + \dots \\
& + \sum_{\substack{i_1 \neq i_2 \neq \dots \neq i_{k-1}=1 \\ i_{k-1}=i_k}}^N \frac{1}{2} \sigma_{\mu_1}^{(i_1)} \otimes \dots \otimes \frac{1}{4} \left(\delta_{\mu_{k-1} \mu_k} \mathbb{1} + i \varepsilon_{\mu_{k-1} \mu_k \mu'} \sigma_{\mu'}^{(i_{k-1})} \right) \\
& = \sum_{i_1 \neq i_2 \neq \dots \neq i_k=1}^N \frac{1}{2} \sigma_{\mu_1}^{(i_1)} \otimes \frac{1}{2} \sigma_{\mu_2}^{(i_2)} \otimes \dots \otimes \frac{1}{2} \sigma_{\mu_k}^{(i_k)} \\
& + \frac{\delta_{\mu_1 \mu_k}}{4} \sum_{\substack{i_1 \neq i_2 \neq \dots \neq i_{k-1}=1 \\ i_1=i_k}}^N \frac{1}{2} \sigma_{\mu_2}^{(i_2)} \otimes \dots \otimes \frac{1}{2} \sigma_{\mu_{k-1}}^{(i_{k-1})} + \frac{i}{2} \varepsilon_{\mu_1 \mu_k \mu'} \sum_{\substack{i_1 \neq i_2 \neq \dots \neq i_{k-1}=1 \\ i_1=i_k}}^N \frac{1}{2} \sigma_{\mu'}^{(i_1)} \otimes \frac{1}{2} \sigma_{\mu_2}^{(i_2)} \otimes \dots \otimes \frac{1}{2} \sigma_{\mu_{k-1}}^{(i_{k-1})} \\
& + \frac{\delta_{\mu_2 \mu_k}}{4} \sum_{\substack{i_1 \neq i_2 \neq \dots \neq i_{k-1}=1 \\ i_2=i_k}}^N \frac{1}{2} \sigma_{\mu_1}^{(i_1)} \otimes \dots \otimes \frac{1}{2} \sigma_{\mu_{k-1}}^{(i_{k-1})} + \frac{i}{2} \varepsilon_{\mu_2 \mu_k \mu'} \sum_{\substack{i_1 \neq i_2 \neq \dots \neq i_{k-1}=1 \\ i_2=i_k}}^N \frac{1}{2} \sigma_{\mu_1}^{(i_1)} \otimes \frac{1}{2} \sigma_{\mu'}^{(i_2)} \otimes \dots \otimes \frac{1}{2} \sigma_{\mu_{k-1}}^{(i_{k-1})} + \dots \\
& + \frac{\delta_{\mu_{k-1} \mu_k}}{4} \sum_{\substack{i_1 \neq i_2 \neq \dots \neq i_{k-1}=1 \\ i_{k-1}=i_k}}^N \frac{1}{2} \sigma_{\mu_1}^{(i_1)} \otimes \dots \otimes \frac{1}{2} \sigma_{\mu_{k-2}}^{(i_{k-2})} + \frac{i}{2} \varepsilon_{\mu_{k-1} \mu_k \mu'} \sum_{\substack{i_1 \neq i_2 \neq \dots \neq i_{k-1}=1 \\ i_{k-1}=i_k}}^N \frac{1}{2} \sigma_{\mu_1}^{(i_1)} \otimes \frac{1}{2} \sigma_{\mu_2}^{(i_2)} \otimes \dots \otimes \frac{1}{2} \sigma_{\mu'}^{(i_{k-1})}.
\end{aligned} \tag{19}$$

In Eq. (19), one can perform a summation of i_j ($j \in \{1, 2, \dots, k\}$) in terms containing the factor $\delta_{\mu_j \mu_k}$. Moreover, given the definition of k -body interaction terms in Eq. (16), each summation term in Eq.(19) can be written as lower-order interaction terms as follows

$$\begin{aligned}
(k-1)! S_{\mu_1 \mu_2 \dots \mu_{k-1}} S_{\mu_k} &= k! S_{\mu_1 \mu_2 \dots \mu_k} + \frac{(k-2)!(N-k+2)}{4} \sum_{i=1}^{k-1} \delta_{\mu_i \mu_k} S_{\mu_1 \dots \hat{\mu}_i \dots \mu_{k-1}} \\
&+ \frac{i(k-1)!}{2} \sum_{i=1}^{k-1} \varepsilon_{\mu_i \mu_k \mu'} S_{\mu_1 \dots \mu_i \rightarrow \mu' \dots \mu_{k-1}},
\end{aligned} \tag{20}$$

where μ_i is omitted from the list in $S_{\mu_1 \dots \hat{\mu}_i \dots \mu_{k-1}}$ and $S_{\mu_1 \dots \mu_i \rightarrow \mu' \dots \mu_{k-1}}$ states that μ_i is replaced by μ' . Hence, the k -body interaction terms can be given as a combination of $(k-1)$ - and $(k-2)$ -body interaction terms

$$S_{\mu_1 \mu_2 \dots \mu_k} = \frac{1}{k} S_{\mu_1 \mu_2 \dots \mu_{k-1}} S_{\mu_k} - \frac{(N-k+2)}{4k(k-1)} \sum_{i=1}^{k-1} \delta_{\mu_i \mu_k} S_{\mu_1 \dots \hat{\mu}_i \dots \mu_{k-1}} - \frac{i}{2k} \sum_{i=1}^{k-1} \varepsilon_{\mu_i \mu_k \mu'} S_{\mu_1 \dots \mu_i \rightarrow \mu' \dots \mu_{k-1}}. \quad (21)$$

To showcase the application of Eq. (21), we consider

- k=2

$$S_{xx} = \frac{1}{2} S_x^2 - \frac{N}{8} \mathbb{1} \quad (22)$$

$$S_{xz} = \frac{1}{2} S_x S_z + \frac{i}{4} S_y \quad (23)$$

- k=3

$$S_{xxx} = \frac{1}{3} S_{xx} S_x - \frac{N-1}{12} S_x \quad (24)$$

$$S_{xxy} = \frac{1}{3} S_{xx} S_y - \frac{i}{3} S_{xz} \quad (25)$$

- k=4

$$S_{xxxx} = \frac{1}{4} S_{xxx} S_x - \frac{N-2}{16} S_{xx} \quad (26)$$

$$S_{xxxx} = \frac{1}{4} S_{xxx} S_z + \frac{3i}{8} S_{xxy} \quad (27)$$

Permutation symmetry

In order to efficiently compute the k -body interaction terms, one can apply the permutationally invariant property of Eq. (21). This means that for each k , one solely needs to compute

$$S_{x^a y^b z^c}, \quad (28)$$

where non-negative integers a, b, c satisfy $a + b + c = k$. For notational simplicity, we will henceforth denote these by S_{abc} . In other words, instead of computing 3^k terms, one needs to compute $\binom{k+2}{2} = (k+2)(k+1)/2$ terms for each k . For example, for

- $k = 1 : S_{100}, S_{010}, S_{001},$
- $k = 2 : S_{200}, S_{020}, S_{002}, S_{110}, S_{101}, S_{011},$
- $k = 3 : S_{300}, S_{030}, S_{003}, S_{210}, S_{201}, S_{021}, S_{120}, S_{102}, S_{012}, S_{111},$
- $k = 4 : S_{400}, S_{040}, S_{004}, S_{310}, S_{301}, S_{220}, S_{202}, S_{211}, S_{121}, S_{112}, S_{130}, S_{103}, S_{022}, S_{031}, S_{013},$

should be computed. By applying the permutation symmetry, Eq. (21) can be recast as follows

$$\begin{aligned} S_{abc} &= \frac{1}{k} S_{ab(c-1)} S_{001} - \frac{(N-k+2)(c-1)}{4k(k-1)} S_{ab(c-2)} - \frac{i}{2k} (a \varepsilon_{xzy} S_{(a-1)(b+1)(c-1)} + b \varepsilon_{yzx} S_{(a+1)(b-1)(c-1)}) \\ &= \frac{1}{k} S_{ab(c-1)} S_{001} - \frac{(N-k+2)(c-1)}{4k(k-1)} S_{ab(c-2)} + \frac{i}{2k} (a S_{(a-1)(b+1)(c-1)} - b S_{(a+1)(b-1)(c-1)}), \end{aligned} \quad (29)$$

where $k = a + b + c$. Substituting $a = b = 0$, yields

$$S_{00c} = \frac{1}{c} S_{00(c-1)} S_{001} - \frac{(N-c+2)}{4c} S_{00(c-2)}. \quad (30)$$

For the case where $c = 0$, Eq. (21) is given by

$$\begin{aligned} S_{ab0} &= \frac{1}{k} S_{a(b-1)0} S_{010} - \frac{(N-k+2)(b-1)}{4k(k-1)} S_{a(b-2)0} - \frac{i}{2k} a \varepsilon_{xyz} S_{(a-1)(b-1)1} \\ &= \frac{1}{k} S_{a(b-1)0} S_{010} - \frac{(N-k+2)(b-1)}{4k(k-1)} S_{a(b-2)0} - \frac{ia}{2k} S_{(a-1)(b-1)1}. \end{aligned} \quad (31)$$

Finally,

$$S_{a00} = \frac{1}{a} S_{(a-1)00} S_{100} - \frac{(N-a+2)}{4a} S_{(a-2)00}. \quad (32)$$

Computing interaction terms in the symmetric subspace

We now compute the k -body interaction terms, Eq. (21), in the symmetric subspace. The operators S_x, S_y, S_z in Eq. (15) are the fundamental representation of SU(2). In the notation introduced in the previous section, these one-body operators correspond to $S_x = S_{100}$, $S_y = S_{010}$, and $S_z = S_{001}$. The higher irreducible representation of SU(2) can be constructed from the product representation of spin- $\frac{1}{2}$. For example, in the case of four spin- $\frac{1}{2}$ systems, the tensor product space is given by

$$\begin{aligned} \mathbb{C}^2 \otimes \mathbb{C}^2 \otimes \mathbb{C}^2 \otimes \mathbb{C}^2 &= (\mathbb{C}^1 \oplus \mathbb{C}^3) \otimes \mathbb{C}^2 \otimes \mathbb{C}^2 \\ &= (\mathbb{C}^2 \oplus \mathbb{C}^2 \oplus \mathbb{C}^4) \otimes \mathbb{C}^2 \\ &= \mathbb{C}^1 \oplus \mathbb{C}^2 \oplus \mathbb{C}^1 \oplus \mathbb{C}^2 \oplus \mathbb{C}^2 \oplus \mathbb{C}^5, \end{aligned} \quad (33)$$

where $\mathbb{C}^1, \mathbb{C}^2, \mathbb{C}^3, \mathbb{C}^4$, and \mathbb{C}^5 correspond to spin-0, spin- $\frac{1}{2}$, spin-1, spin- $\frac{3}{2}$, and spin-2 representation, respectively. The spin- S representation corresponds to $(2S+1)$ -dimensional vector space in which $m = \{-S, -S+1, \dots, S-1, S\}$. In this representation, the basis states are the common eigenstates of S_z and S^2 which is defined as

$$S^2 = S_x^2 + S_y^2 + S_z^2. \quad (34)$$

Hence

$$S_z |S, m\rangle = m |S, m\rangle, \quad (35)$$

$$S^2 |S, m\rangle = S(S+1) |S, m\rangle. \quad (36)$$

Introducing *raising* and *lowering* operator S_+ and S_- , respectively, as follows

$$S_{\pm} |S, m\rangle = \sqrt{(S \mp m)(S \pm m + 1)} |S, m \pm 1\rangle, \quad (37)$$

leads to

$$S_x = \frac{1}{2} (S_+ + S_-), \quad (38)$$

$$S_y = \frac{1}{2i} (S_+ - S_-). \quad (39)$$

This representation simplifies the computation of k -body interaction terms in the symmetric subspace. The symmetric subspace can be spanned by the Dicke basis $\{|D_N^0\rangle, |D_N^1\rangle, \dots, |D_N^N\rangle\}$ in $(N+1)$ dimensional subspace. This subspace corresponds to the irreducible representation of spin- S with dimension $(2S+1)$. Therefore, any arbitrary quantum state, $|\psi_0\rangle$, in the symmetric subspace can be written as follows

$$|\psi\rangle = \sum_{n=0}^N C_n |D_N^n\rangle \equiv \sum_{m=-N/2}^{N/2} \alpha_m \left| \frac{N}{2}, m \right\rangle, \quad (40)$$

where $C_n, \alpha_m \in \mathbb{C}$. For instance in the case of $N = 2$:

$$\begin{aligned} \frac{1}{2} \otimes \frac{1}{2} &\stackrel{(33)}{=} 0 \oplus 1 \\ &= \begin{pmatrix} 0 & \vdots & & \\ \cdots & \cdots & \cdots & \\ & \vdots & & 1_{3 \times 3} \\ & \vdots & & \end{pmatrix}, \end{aligned} \quad (41)$$

for $S = 1, m = \{-1, 0, +1\}$. The symmetric subspace can be constructed with the following bases

$$\begin{aligned} |D_2^0\rangle &= |00\rangle, \\ |D_2^1\rangle &= \frac{1}{\sqrt{2}}(|10\rangle + |01\rangle), \\ |D_2^2\rangle &= |11\rangle, \end{aligned}$$

which is a 3-dimensional space. This shows that the spin-1 representation can be utilized to represent the symmetric subspace.

The next step is finding the representation of one-body interaction terms, Eq. (14), in spin- S representation (or symmetric subspace). These are given by

$$\left\langle \frac{N}{2}, m' \middle| S_x \middle| \frac{N}{2}, m \right\rangle = \frac{1}{2} \left[\sqrt{\left(\frac{N}{2} - m\right)\left(\frac{N}{2} + m + 1\right)} \delta_{m', m+1} + \sqrt{\left(\frac{N}{2} + m\right)\left(\frac{N}{2} - m + 1\right)} \delta_{m', m-1} \right], \quad (42)$$

$$\left\langle \frac{N}{2}, m' \middle| S_y \middle| \frac{N}{2}, m \right\rangle = \frac{1}{2i} \left[\sqrt{\left(\frac{N}{2} - m\right)\left(\frac{N}{2} + m + 1\right)} \delta_{m', m+1} - \sqrt{\left(\frac{N}{2} + m\right)\left(\frac{N}{2} - m + 1\right)} \delta_{m', m-1} \right], \quad (43)$$

$$\left\langle \frac{N}{2}, m' \middle| S_z \middle| \frac{N}{2}, m \right\rangle = m \delta_{m', m}, \quad (44)$$

where $m', m \in \{-N/2, -N/2+1, \dots, N/2-1, N/2\}$. For $N = 2$, the spin-1 representations of one-body interaction terms are derived as follows

$$S_x = \frac{1}{\sqrt{2}} \begin{pmatrix} 0 & 1 & 0 \\ 1 & 0 & 1 \\ 0 & 1 & 0 \end{pmatrix}, \quad (45)$$

$$S_y = \frac{1}{i\sqrt{2}} \begin{pmatrix} 0 & 1 & 0 \\ -1 & 0 & 1 \\ 0 & -1 & 0 \end{pmatrix}, \quad (46)$$

$$S_z = \begin{pmatrix} 1 & 0 & 0 \\ 0 & 0 & 0 \\ 0 & 0 & -1 \end{pmatrix}. \quad (47)$$

Substituting Eqs. (45, 46, 47) in Eq. (34), yields

$$S^2 = \begin{pmatrix} 2 & 0 & 0 \\ 0 & 2 & 0 \\ 0 & 0 & 2 \end{pmatrix}, \quad (48)$$

which is compatible with Eq. (36) for $S = 1$

$$\left\langle \frac{N}{2}, m' \middle| S^2 \middle| \frac{N}{2}, m \right\rangle = S(S+1) \delta_{m', m}. \quad (49)$$

PRELIMINARIES ON THE SYMMETRIC SUBSPACE

This appendix presents essential background on the symmetric subspace that is necessary for deriving subsequent results. The symmetric subspace can be expanded by the so-called Dicke states. In the computational basis, an N -qubit Dicke state with n excitations is given by

$$|D_N^n\rangle = \frac{1}{\sqrt{\binom{N}{n}}} \sum_{\mathbf{i}} \delta(|\mathbf{i}| - n) |\mathbf{i}\rangle, \quad (50)$$

where $\mathbf{i} = i_0 i_1 \cdots i_{N-1}$ in which $i_\gamma \in \{0, 1\}$ and $|\mathbf{i}|$ denotes the number of ones in the binary representation. Any arbitrary quantum state, $|\psi\rangle$, can be written in the symmetric subspace as follows

$$|\psi\rangle = \sum_{n=0}^N C_n |D_N^n\rangle. \quad (51)$$

where $C_n \in \mathbb{C}$. To reduce the complexity of the problem from 2^N in the computational basis to $(N + 1)$ within the symmetric subspace (spanned by the Dicke states defined in Eq. (50)), one can define the following projector operator

$$\mathcal{P} = \mathcal{V}^\dagger \mathcal{V}, \quad (52)$$

where

$$\mathcal{V} = \sum_{n=0}^N |n\rangle \langle D_N^n|, \quad (53)$$

in which $|n\rangle$ and $|D_N^n\rangle$ are in the symmetric subspace (($N + 1$)-dimension) and the computational space (2^N -dimension), respectively, and satisfies $\mathcal{V}\mathcal{V}^\dagger = \mathbb{1}_{(N+1) \times (N+1)}$.

An alternative definition of the symmetric subspace can be given in terms of permutation operators [66]. The symmetric group \mathcal{S}_N consisting of permutations of N elements, where

$$\sigma : \{1, 2, \dots, N\} \rightarrow \{1, 2, \dots, N\}, \quad \forall \sigma \in \mathcal{S}_N. \quad (54)$$

One can define the permutation matrix U_σ which satisfies

$$U_\sigma (|\psi_1\rangle \otimes |\psi_2\rangle \otimes \cdots \otimes |\psi_N\rangle) = |\psi_{\sigma^{-1}(1)}\rangle \otimes |\psi_{\sigma^{-1}(2)}\rangle \otimes \cdots \otimes |\psi_{\sigma^{-1}(N)}\rangle. \quad (55)$$

Specifically, let us define the symmetric subspace as the space that remains invariant under the action of any permutation matrix U_σ as

$$\text{Sym} := \{|\psi\rangle \mid U_\sigma |\psi\rangle = |\psi\rangle, \forall \sigma \in \mathcal{S}_N\}. \quad (56)$$

Hence, one can define an alternative definition of the projector operator onto the symmetric subspace, Eq. (52), as follows

$$\mathcal{P} = \frac{1}{N!} \sum_{\sigma \in \mathcal{S}_N} U_\sigma. \quad (57)$$

It is straightforward to check that Eq. (57) satisfies all the conditions of projector operation.

COMPUTING THE QFI FOR THE UNITARY EVOLUTION IN THE SYMMETRIC SUBSPACE

Here, we derive a general formula for calculating the QFI in the case of unitary evolution in the symmetric subspace. Computing the QFI in the symmetric subspace simplifies calculations and allows us to consider larger N . Consider the evolution where the unknown parameter θ is encoded via local unitary evolution $U(\theta) = e^{-iG(\theta)}$ in which $G(\theta)$ is a Hermitian operator. Hence, the sampling operator can be defined as

$$\mathbf{U}(\theta) = U(\theta)^{\otimes N}. \quad (58)$$

It is straightforward to check that for any 2×2 unitary evolution like

$$U(\theta) = \begin{pmatrix} \mathcal{U}_{00}(\theta) & \mathcal{U}_{01}(\theta) \\ \mathcal{U}_{10}(\theta) & \mathcal{U}_{11}(\theta) \end{pmatrix}, \quad (59)$$

the representation of the sampling operator, $\mathbf{U}(\theta)$ (Eq. (58)), in the computational basis is given by

$$\mathbf{U}(\theta) = \sum_{\mathbf{i}, \mathbf{j}} |\mathbf{i}\rangle \langle \mathbf{j}| \prod_{\gamma=0}^1 \mathcal{U}_{i_\gamma, j_\gamma}(\theta). \quad (60)$$

Theorem 1 *The sampling operator $\mathbf{U}(\theta)$ commutes with the projector operator onto the symmetric subspace, \mathcal{P} ,*

$$[\mathbf{U}(\theta), \mathcal{P}] = 0. \quad (61)$$

Proof:

Lemma 1 *The sampling operator $\mathbf{U}(\theta)$ commutes with permutation matrix U_σ , $\forall \sigma \in \mathcal{S}_N$ (Eq. (55)).*

Proof: Let consider

$$\begin{aligned} U_\sigma \mathbf{U}(\theta) (|\psi_1\rangle \otimes |\psi_2\rangle \otimes \cdots \otimes |\psi_N\rangle) &\stackrel{(58)}{=} U_\sigma U(\theta)^{\otimes N} (|\psi_1\rangle \otimes |\psi_2\rangle \otimes \cdots \otimes |\psi_N\rangle) \\ &= U_\sigma (U(\theta) |\psi_1\rangle \otimes U(\theta) |\psi_2\rangle \otimes \cdots \otimes U(\theta) |\psi_N\rangle) \\ &\stackrel{(55)}{=} |\psi_{\sigma^{-1}(1)}(\theta)\rangle \otimes |\psi_{\sigma^{-1}(2)}(\theta)\rangle \otimes \cdots \otimes |\psi_{\sigma^{-1}(N)}(\theta)\rangle \\ &= U(\theta) |\psi_{\sigma^{-1}(1)}\rangle \otimes U(\theta) |\psi_{\sigma^{-1}(2)}\rangle \otimes \cdots \otimes U(\theta) |\psi_{\sigma^{-1}(N)}\rangle \\ &= \mathbf{U}(\theta) U_\sigma (|\psi_1\rangle \otimes |\psi_2\rangle \otimes \cdots \otimes |\psi_N\rangle). \end{aligned} \quad (62)$$

Since Eq. (62) holds for any arbitrary $|\psi_1\rangle, |\psi_2\rangle, \dots, |\psi_N\rangle$, then

$$[\mathbf{U}(\theta), U_\sigma] = 0, \quad \forall \sigma \in \mathcal{S}_N. \quad (63)$$

Therefore, Eqs. (57) and (63) complete the proof. ■

Corollary 1 Since $[\mathbf{U}(\theta), \mathcal{P}] = 0$, then

$$[\partial_\theta \mathbf{U}(\theta), \mathcal{P}] = 0. \quad (64)$$

To compute the QFI, Eq. (2), let us consider the case in which the sampling operator is given by Eq. (58) and the initial state $|\psi_0\rangle$ is chosen from the symmetric subspace. Hence

$$|\psi_\theta\rangle = \mathbf{U}(\theta) |\psi_0\rangle, \quad (65)$$

and

$$|\psi_0\rangle = \mathcal{P} |\psi_0\rangle. \quad (66)$$

Whence

$$|\psi_\theta\rangle = \mathbf{U}(\theta) \mathcal{P} |\psi_0\rangle, \quad (67)$$

$$|\partial_\theta \psi_\theta\rangle = \partial_\theta \mathbf{U}(\theta) \mathcal{P} |\psi_0\rangle. \quad (68)$$

Substituting Eqs. (67,68) in the QFI relation, Eq. (2), yields to the QFI of the pure state in the symmetric subspace

$$\begin{aligned}
\mathcal{F}^{(\text{sym.})}[\psi_\theta] &= 4 \left(\langle \psi_0 | \mathcal{P} \partial_\theta \mathbf{U}^\dagger(\theta) \partial_\theta \mathbf{U}(\theta) \mathcal{P} | \psi_0 \rangle - \langle \psi_0 | \mathcal{P} \mathbf{U}^\dagger(\theta) \partial_\theta \mathbf{U}(\theta) \mathcal{P} | \psi_0 \rangle \langle \psi_0 | \mathcal{P} \partial_\theta \mathbf{U}^\dagger(\theta) \mathbf{U}(\theta) \mathcal{P} | \psi_0 \rangle \right) \\
&\stackrel{(\mathcal{P}^2 = \mathcal{P})}{=} 4 \left(\langle \psi_0 | \mathcal{P} \partial_\theta \mathbf{U}^\dagger(\theta) \partial_\theta \mathbf{U}(\theta) \mathcal{P} | \psi_0 \rangle \right) \\
&\quad - 4 \left(\langle \psi_0 | \mathcal{P} \mathbf{U}^\dagger(\theta) \partial_\theta \mathbf{U}(\theta) \mathcal{P} | \psi_0 \rangle \langle \psi_0 | \mathcal{P} \partial_\theta \mathbf{U}^\dagger(\theta) \mathbf{U}(\theta) \mathcal{P} | \psi_0 \rangle \right) \\
&\stackrel{(61),(64)}{=} 4 \left(\langle \psi_0 | \mathcal{P} \partial_\theta \mathbf{U}^\dagger(\theta) \mathcal{P} \partial_\theta \mathbf{U}(\theta) | \psi_0 \rangle \right) \\
&\quad - 4 \left(\langle \psi_0 | \mathcal{P} \mathbf{U}^\dagger(\theta) \mathcal{P} \partial_\theta \mathbf{U}(\theta) | \psi_0 \rangle \langle \psi_0 | \mathcal{P} \partial_\theta \mathbf{U}^\dagger(\theta) \mathbf{U}(\theta) \mathcal{P} | \psi_0 \rangle \right) \\
&\stackrel{(52)}{=} 4 \left(\langle \phi_0 | \partial_\theta \mathbf{W}^\dagger(\theta) \partial_\theta \mathbf{W}(\theta) | \phi_0 \rangle - \langle \phi_0 | \mathbf{W}^\dagger(\theta) \partial_\theta \mathbf{W}(\theta) | \phi_0 \rangle \langle \phi_0 | \partial_\theta \mathbf{W}^\dagger(\theta) \mathbf{W}(\theta) | \phi_0 \rangle \right), \tag{69}
\end{aligned}$$

where

$$|\phi_0\rangle := \mathcal{V}|\psi_0\rangle, \tag{70}$$

$$\mathbf{W}(\theta) := \mathcal{V} \mathbf{U}(\theta) \mathcal{V}^\dagger. \tag{71}$$

As explicitly shown by Eq. (70), $|\phi_0\rangle$ belongs to the $(N + 1)$ -dimensional symmetric subspace. Hence, it can be written in the following form

$$|\phi_0\rangle = \sum_{n=0}^N \alpha_n |n\rangle, \tag{72}$$

where $\alpha_n \in \mathbb{C}$ and $\sum_n |\alpha_n|^2 = 1$. Crucially, calculating the QFI within the symmetric subspace, Eq. (69), requires computing $\mathbf{W}(\theta)$, Eq. (71). Indeed, this operator denotes the projection of the sampling operator, $\mathbf{U}(\theta)$, from the 2^N -dimensional computational basis onto the $(N + 1)$ -dimensional symmetric subspace. The explicit derivation of $\mathbf{W}(\theta)$ is as follows

$$\begin{aligned}
\mathbf{W}(\theta) &= \mathcal{V} \mathbf{U}(\theta) \mathcal{V}^\dagger \\
&\stackrel{(53)}{=} \sum_{n,m=0}^N C_{mn} |m\rangle \langle n|, \tag{73}
\end{aligned}$$

where

$$C_{mn} := \langle D_N^m | \mathbf{U}(\theta) | D_N^n \rangle. \tag{74}$$

Substituting Eqs. (50,60) in Eq. (74), gives

$$C_{mn} = \sum_{m,n=0}^N \frac{1}{\sqrt{\binom{N}{m} \binom{N}{n}}} \sum_{\mathbf{i},\mathbf{j}} \delta(|\mathbf{i}| - m) \delta(|\mathbf{j}| - n) \prod_{\gamma=0}^1 \mathcal{U}_{i_\gamma, j_\gamma}(\theta). \tag{75}$$

In order to compute C_{mn} , we define four vectors ω_i for $i \in \{0, 1, 2, 3\}$

$$\omega_0 = \begin{pmatrix} 0 \\ 0 \end{pmatrix}, \tag{76}$$

$$\omega_1 = \begin{pmatrix} 0 \\ 1 \end{pmatrix}, \tag{77}$$

$$\omega_2 = \begin{pmatrix} 1 \\ 0 \end{pmatrix}, \tag{78}$$

$$\omega_3 = \begin{pmatrix} 1 \\ 1 \end{pmatrix}. \tag{79}$$

The first and second entries of ω_i correspond to elements from strings \mathbf{i} and \mathbf{j} respectively. These vectors are used to determine $|\mathbf{i}|$ and $|\mathbf{j}|$ and to select the appropriate $\mathcal{U}_{i_\gamma, j_\gamma}$. Therefore, one can obtain

$$|\mathbf{i}| = \bar{\omega}_2 + \bar{\omega}_3, \quad (80)$$

$$|\mathbf{j}| = \bar{\omega}_1 + \bar{\omega}_3, \quad (81)$$

where $\bar{\omega}_i$ counts the number of times where ω_i appears in the \mathbf{i} and \mathbf{j} strings. For example in the case where

$$\begin{aligned} \mathbf{i} &= 0 \quad 0 \quad 1 \quad 0 \quad 1, \\ \mathbf{j} &= \underbrace{0}_{\omega_0} \quad \underbrace{0}_{\omega_0} \quad \underbrace{0}_{\omega_2} \quad \underbrace{1}_{\omega_1} \quad \underbrace{1}_{\omega_3}, \end{aligned}$$

$\bar{\omega}_0 = 2$, $\bar{\omega}_1 = 1$, $\bar{\omega}_2 = 1$, and $\bar{\omega}_3 = 1$. Then $\vec{\omega} := (\bar{\omega}_0, \bar{\omega}_1, \bar{\omega}_2, \bar{\omega}_3) = (2, 1, 1, 1)$.

Since $N = \sum_{i=0}^3 \bar{\omega}_i$, one needs to count the number of different partitions of N where the $\{\omega_i\}$'s are the parts by using

$$\binom{N}{\bar{\omega}_0} \binom{N - \bar{\omega}_0}{\bar{\omega}_1} \binom{N - \bar{\omega}_0 - \bar{\omega}_1}{\bar{\omega}_2} \binom{N - \bar{\omega}_0 - \bar{\omega}_1 - \bar{\omega}_2}{\bar{\omega}_3} = \frac{N!}{\bar{\omega}_0! \bar{\omega}_1! \bar{\omega}_2! \bar{\omega}_3!}. \quad (82)$$

Applying these consideration, Eq. (75) yields

$$\mathcal{C}_{mn} = \sum_{m,n=0}^N \sum_{\vec{\omega} \vdash N} \frac{N!}{\bar{\omega}_0! \bar{\omega}_1! \bar{\omega}_2! \bar{\omega}_3!} \frac{\delta(\bar{\omega}_2 + \bar{\omega}_3 - m) \delta(\bar{\omega}_1 + \bar{\omega}_3 - n)}{\sqrt{\binom{N}{m} \binom{N}{n}}} \mathcal{U}_{00}^{\bar{\omega}_0}(\theta) \mathcal{U}_{01}^{\bar{\omega}_1}(\theta) \mathcal{U}_{10}^{\bar{\omega}_2}(\theta) \mathcal{U}_{11}^{\bar{\omega}_3}(\theta), \quad (83)$$

and its first derivative with respect to the unknown parameter is given by

$$\begin{aligned} \partial_\theta \mathcal{C}_{mn} &= \sum_{m,n=0}^N \sum_{\vec{\omega} \vdash N} \frac{N!}{\bar{\omega}_0! \bar{\omega}_1! \bar{\omega}_2! \bar{\omega}_3!} \frac{\delta(\bar{\omega}_2 + \bar{\omega}_3 - m) \delta(\bar{\omega}_1 + \bar{\omega}_3 - n)}{\sqrt{\binom{N}{m} \binom{N}{n}}} \\ &\quad \left(\bar{\omega}_0 \partial_\theta \mathcal{U}_{00}(\theta) \mathcal{U}_{00}^{\bar{\omega}_0-1}(\theta) \mathcal{U}_{01}^{\bar{\omega}_1}(\theta) \mathcal{U}_{10}^{\bar{\omega}_2}(\theta) \mathcal{U}_{11}^{\bar{\omega}_3}(\theta) + \bar{\omega}_1 \partial_\theta \mathcal{U}_{01}(\theta) \mathcal{U}_{00}^{\bar{\omega}_0}(\theta) \mathcal{U}_{01}^{\bar{\omega}_1-1}(\theta) \mathcal{U}_{10}^{\bar{\omega}_2}(\theta) \mathcal{U}_{11}^{\bar{\omega}_3}(\theta) \right. \\ &\quad \left. \bar{\omega}_2 \partial_\theta \mathcal{U}_{10}(\theta) \mathcal{U}_{00}^{\bar{\omega}_0}(\theta) \mathcal{U}_{01}^{\bar{\omega}_1}(\theta) \mathcal{U}_{10}^{\bar{\omega}_2-1}(\theta) \mathcal{U}_{11}^{\bar{\omega}_3}(\theta) + \bar{\omega}_3 \partial_\theta \mathcal{U}_{11}(\theta) \mathcal{U}_{00}^{\bar{\omega}_0}(\theta) \mathcal{U}_{01}^{\bar{\omega}_1}(\theta) \mathcal{U}_{10}^{\bar{\omega}_2}(\theta) \mathcal{U}_{11}^{\bar{\omega}_3-1}(\theta) \right) \end{aligned} \quad (84)$$

where $\vec{\omega} \vdash N$ indicates that N is partitioned as $\vec{\omega}$. By exploiting Eqs. (72,73,83,84), Eq. (69) can be cast in this form

$$\mathcal{F}^{(\text{sym.})} [|\psi_\theta\rangle] = 4 \left[\sum_{m,n,l=0}^N \alpha_m^* \alpha_n (\partial_\theta \mathcal{C}_{lm})^* \partial_\theta \mathcal{C}_{ln} - \left| \sum_{m,n,l=0}^N \alpha_m^* \alpha_n \mathcal{C}_{lm}^* \partial_\theta \mathcal{C}_{ln} \right|^2 \right]. \quad (85)$$

UPPER BOUND ON THE QFI—DERIVATION OF EQ. (4)

Here we derive an upper bound on the QFI of unitary evolution and a pure probe state. The approach is nearly the same as the one used in Ref. [67]. Let us begin by recalling the closed-form formula of the QFI for PDH

$$\mathcal{F}[|\psi_\theta\rangle] = 4\Delta^2 \mathbf{K}_\theta = 4(\langle \mathbf{K}_\theta^2 \rangle - \langle \mathbf{K}_\theta \rangle^2). \quad (86)$$

To provide an upper bound on the variance in Eq. (86), one can exploit the operator seminorm with following properties

- **(P1):** for Hermitian operator \mathcal{A} is defined as $\lambda_M(\mathcal{A}) - \lambda_m(\mathcal{A})$,
- **(P2):** it is called seminorm (not a norm) because for $\mathcal{A} = \alpha \mathbf{1}$, $\|\mathcal{A}\|_{\text{sn}} = 0$, but $\mathcal{A} \neq 0$, unless $\alpha \neq 0$,
- **(P3): triangle inequality (commuting operators):** If $[\mathcal{A}, \mathcal{B}] = 0$, then $\|\mathcal{A} + \mathcal{B}\|_{\text{sn}} = \|\mathcal{A}\|_{\text{sn}} + \|\mathcal{B}\|_{\text{sn}}$,
- **(P4): unitary invariance:** $\|U \mathcal{A} U^\dagger\|_{\text{sn}} = \|\mathcal{A}\|_{\text{sn}}$ for any unitary U .

Since \mathbf{K}_θ is a Hermitian operator, Eq. (86) yields

$$\mathcal{F}[|\psi_\theta\rangle] \leq \|\mathbf{K}_\theta\|_{\text{sn}}^2. \quad (87)$$

In order to upper bound Eq. (87), we start from the definition of \mathbf{K}_θ

$$\begin{aligned} \|\mathbf{K}_\theta\|_{\text{sn}} &= \left\| i\partial_\theta \mathbf{U}_\theta \mathbf{U}_\theta^\dagger \right\|_{\text{sn}} \\ &= \left\| i\partial_\theta U_\theta^{\otimes N} U_\theta^{\otimes N\dagger} \right\|_{\text{sn}} \\ &= \left\| i \left(\sum_{i=1}^N U_\theta \otimes U_\theta \otimes \cdots \otimes \underbrace{\partial_\theta U_\theta}_{i^{\text{th}}} \otimes \cdots U_\theta \right) U_\theta^{\otimes N\dagger} \right\|_{\text{sn}} \\ &= \left\| \sum_{i=1}^N \mathbb{1} \otimes \mathbb{1} \otimes \cdots \otimes \underbrace{i\partial_\theta U_\theta U_\theta^\dagger}_{i^{\text{th}}} \otimes \cdots \mathbb{1} \right\|_{\text{sn}} \\ &\stackrel{(\text{P3})}{=} \sum_{i=1}^N \left\| \mathbb{1} \otimes \mathbb{1} \otimes \cdots \otimes K_\theta \otimes \cdots \mathbb{1} \right\|_{\text{sn}} \\ &= N\|K_\theta\|_{\text{sn}}. \end{aligned} \quad (88)$$

From whence

$$\mathcal{F}[|\psi_\theta\rangle] = 4\Delta^2 \mathbf{K}_\theta \leq \|\mathbf{K}_\theta\|_{\text{sn}}^2 = N^2\|K_\theta\|_{\text{sn}}^2. \quad (89)$$

To finish the section, let us comment on the saturation of the bound Eq. (89). Direct computation shows that states of the form $|\psi_\theta\rangle = (|\lambda_M(\theta)\rangle + |\lambda_m(\theta)\rangle)/\sqrt{2}$, where $|\lambda_{M/m}(\theta)\rangle$ are respectively the max/min eigenvectors of \mathbf{K}_θ saturate the bound. Moreover, since $\mathbf{K}_\theta = \sum_{i=1}^N K_\theta^{(i)}$, where $K_\theta^{(i)}$ only acts nontrivially on qubit i , $|\lambda_{M/m}(\theta)\rangle = |\lambda_{M/m}(\theta)\rangle^{\otimes N}$, where $|\lambda_{M/m}(\theta)\rangle$ are respectively the max/min eigenvectors of K_θ .

Figure (5) presents the results of utilizing our method to identify the optimal probe states that saturate the bound in Eq. (89) for the case where $G_\theta = \cos(\theta)\sigma_z + \sin(\theta)\sigma_x$. At first glance, Fig. (5) may suggest that the upper bound is saturated only for even values of N . However, this apparent behavior arises due to the randomness of the sampled coefficients and does not reflect a fundamental limitation. In Fig. (6), we go beyond random sampling by directly optimizing the QFI and find that for all values of N , there exist corresponding system's Hamiltonian whose ground states saturate the upper bound.

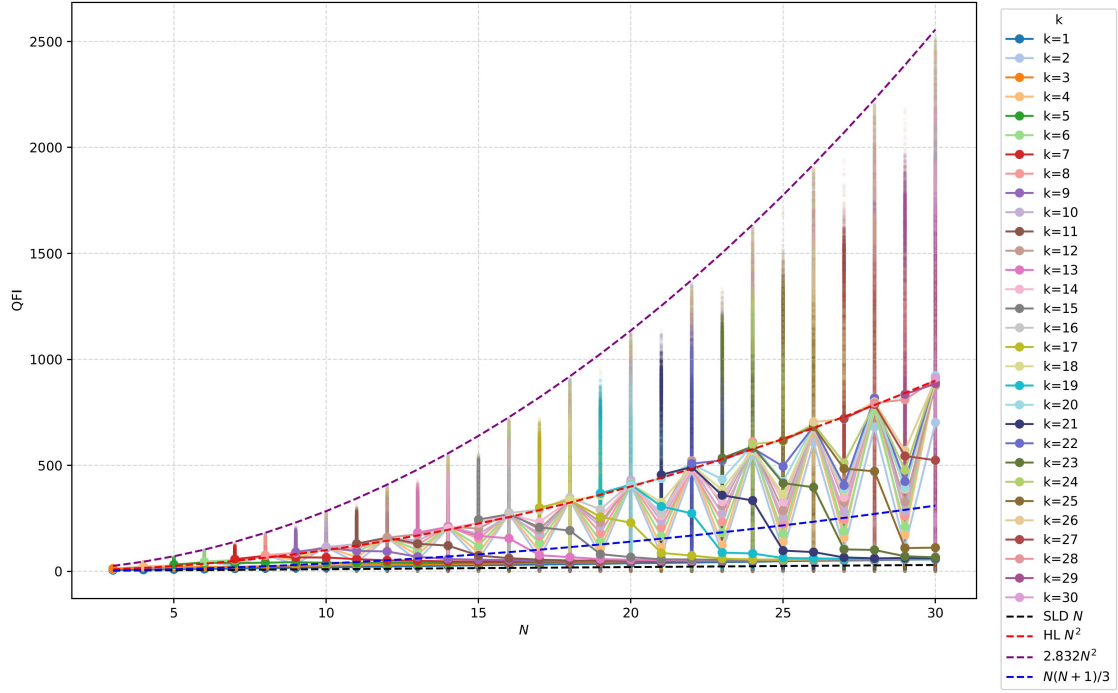


Figure 5. The QFI as a function of N for the case where the encoding Hamiltonian is $G_\theta = \cos(\theta)\sigma_z + \sin(\theta)\sigma_x$. The probe states are the ground states of system's Hamiltonian, constructed with randomly sampled coefficients drawn from a normal distribution $\mathcal{N}(0, 1)$, for various k -body interaction terms. For each value of k , 2000 random instances were sampled.

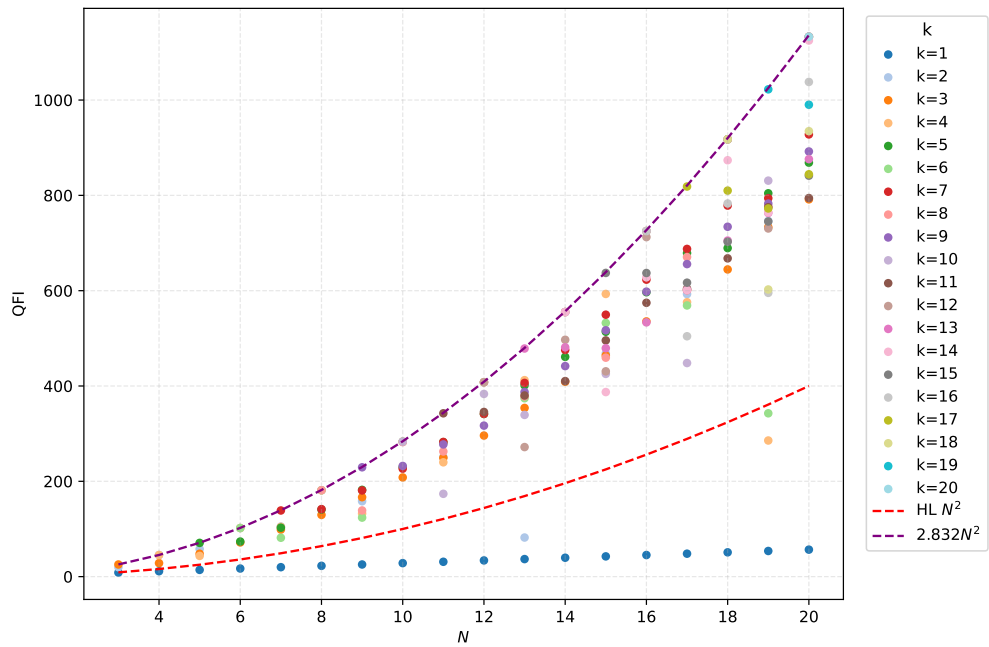


Figure 6. The QFI as a function of N for the case where the encoding Hamiltonian is $G_\theta = \cos(\theta)\sigma_z + \sin(\theta)\sigma_x$. By optimization, For all values of N , the upper bound in Eq. (89) is saturable.